

Singularities in droplet pinching with vanishing viscosity

Jens Eggers

Universität Gesamthochschule Essen, Fachbereich Physik,
45117 Essen, Germany

Abstract

A slender-jet model for the pinching of a liquid column is considered in the limit of vanishing viscosity. We find the model to develop a singularity in the gradients of the local radius and the velocity at a finite thread radius, so it does not describe breakup. However, the observed steepening of the profile corresponds to experiments and simulations with fluids at low viscosity. The singularity has similarity form, which we compute analytically. The result agrees well with numerical simulations of the model equations.

I. INTRODUCTION

Considerable attention has been devoted recently to the breakup of an axisymmetric column of fluid [1–5]. The breakup is driven by surface tension forces, which reduce the surface area by contracting the fluid thread until its radius goes to zero at a point. As a typical example, we show a drop of water falling from a faucet in Fig.1 [6,7].

Close to the point of breakup, the interface looks like a cone attached to a nearly flat interface. This is characteristic for low viscosity fluids, where viscosity is important only in a small spatial region around the point of breakup. Details of the initial conditions or external forces like gravity are believed to have little impact on the very localized behavior close to pinch-off. Indeed experiments with or without gravity and for a variety of nozzle diameters show very similar shapes [4]. This is because surface tension forces become very strong near pinching, and drive very small amounts of fluid. Thus the very rapid motion close to breakup is separated dynamically from the motion on the scale of the nozzle diameter both in space and time. A proper measure of length and time are the *local* scales

$$\ell_\nu = (\nu^2 \rho) / \gamma, \quad t_\nu = (\nu^3 \rho^2) / \gamma^2, \quad (1)$$

which only depend on the properties of the fluid. Here ν is the kinematic viscosity, γ the surface tension, and ρ is the density of the fluid. In the case that the minimum radius h_{min} of the fluid neck is much smaller than ℓ_ν , a universal pinching solution has been observed [1,3]. As the radius of the fluid neck goes to zero, surface tension, viscous, and inertial forces are of the same order.

For a low viscosity fluid like water, however, ℓ_ν is only 100 Å, so this asymptotic solution is hardly of relevance experimentally. Accordingly, it would be extremely desirable to develop a similarity theory valid in the range $h_{min} \gg \ell_\nu$. Assuming that all flow features of a hypothetical Navier-Stokes solution are of the same order as h_{min} , it is tempting to look at solutions of the inviscid (Euler) equation for that regime. Unfortunately, the Euler equation is known [8] to exhibit spurious blow-up of the local vorticity, even starting from smooth

initial data. This problem can be avoided by only considering the subclass of solutions which are irrotational, and are thus described by potential flow. Numerical simulations of inviscid, irrotational flow driven by surface tension were used by a number of authors [9,10] to describe pinching. After the minimum radius has reached a value of about 1/20 of its initial value, all simulations show an *overturning* of the profile. This means that the neck radius $h(z)$ is no longer a single-valued function of the position along the axis z . Recently [5] it was shown that this overturning can be understood as the convergence onto a universal similarity solution of the inviscid, irrotational equations. Similar findings were reported by Chen and Steen [11] for the related problem of a soap film which drives a flow in the surrounding air. Neglecting the inertia of the film, this corresponds to the motion of two fluids of equal density with surface tension between them.

The fundamental question thus remains whether viscosity can really be neglected. A Navier-Stokes computation at low viscosities [12] showed no signs of overturning, although the initial neck radius was $4 \cdot 10^4 \ell_\nu$. Experimentally, [6,13] there is also no sign of overturning even in water, an event that would show up in the side view as a flat wall perpendicular to the axis. Clearly, other and more detailed simulations of low-viscosity fluids are needed to confirm this, but there is reasonable concern that the assumption behind the inviscid-flow calculations are fundamentally flawed.

In [13] we use a slender-jet model, originally developed in [7], to investigate the possible effect of a very small amount of viscosity on the pinching of a liquid thread. The model [16,7] can be shown to capture all the leading-order contributions to the jet dynamics below the viscous scale ℓ_ν . In addition, it was demonstrated in [7] that by including the full mean curvature as a higher-order contribution to the pressure, the model can reproduce experimental profiles even when $h_{min} \gg \ell_\nu$. As an example, in Fig.1 a few profiles calculated from the slender jet model are superimposed on the experimental picture [7]. Thus although the model is formally not valid in the presence of large gradients, it is interesting to understand the limit of small viscosity in this case since it turns out to be analytically tractable.

In [13] we show numerically that the slender-jet model for small viscosity develops very

sharp gradients both in the local radius and the velocity field. This causes viscous effects to become important in a very small region where gradients are large even though the minimum radius h_{min} is still much larger than ℓ_ν . Clearly this is because the small-viscosity dynamics produces flow features which are much smaller than h_{min} .

In the present paper we show that the inviscid equations indeed have a singularity which leads to a blow-up of gradients in finite time. This has been done by explicitly constructing a similarity solution which solves the equations for $\nu = 0$. We extend the numerical code used previously in [13] to even smaller viscosities to show that in the limit $\nu \rightarrow 0$ of small viscosities the slender-jet equations always select this inviscid singularity. The blow-up occurs while the minimum radius is still finite and an analytical description of the local profiles is given. In particular the inviscid equations are not able to describe breakup, although the full curvature term is kept.

If one follows the above argument, inviscid scaling theories [5,14,15] may fail even for arbitrarily small ℓ_ν . On the other hand, our analysis is based on a simplified one-dimensional description of a liquid thread, which represents a serious shortcoming compared to the three-dimensional axisymmetric representation of [5]. In particular, overturning cannot be described within the model. To settle the question whether inviscid scaling is consistent, a very careful comparison with both experiment [6,13] and full Navier-Stokes simulations [12] is necessary. In particular more carefully resolved Navier-Stokes computations are highly desirable.

In the next section we introduce the one-dimensional slender-jet model which forms the basis of our analytical description of the inviscid singularity. We then present conclusive numerical evidence for the existence of a inviscid singularity at a time t_c . Derivatives of the surface profile and of the velocity diverge like a power law as function of $t_c - t$. In the third section we present an analytical theory of the inviscid singularity. The resulting surface profiles agree well with numerical simulations.

II. MODEL AND SIMULATIONS

The main assumption underlying the model of axisymmetric free-surface flow to be considered here is that the fluid motion is directed mostly in the axial direction. This allows to set up an asymptotic expansion [16] in the thread radius, which at leading order gives equations for the radius $h(z, t)$ of the thread and for the velocity $v(z, t)$, which only depend on the axial coordinate z . In what follows we will deal with the model introduced in [7],

$$\partial_t h = -vh_z - v_z h/2, \tag{2a}$$

$$\partial_t v = -vv_z - p_z + \frac{3\nu}{LU} \frac{(h^2 v_z)_z}{h^2}, \tag{2b}$$

$$p = \frac{1}{h(1 + h_z^2)^{1/2}} - \frac{h_{zz}}{(1 + h_z^2)^{3/2}}, \tag{2c}$$

where the index refers to differentiation with respect to the variable. The fields $h(z, t)$ and $v(z, t)$ have been non-dimensionalized using some fixed length scale L of the problem (like the radius of a nozzle). The length L can be combined with surface tension γ and density ρ to make up a time scale $T = (\rho L^3 / \gamma)^{1/2}$ and a velocity scale $U = L/T$. Every quantity to follow will be non-dimensionalized using these units.

Equation (2a) expresses mass conservation for a radially uniform velocity field. Conservation of momentum (2b) not surprisingly has the form of Burgers' equation in the inviscid limit, driven by surface tension forces which are proportional to the mean curvature (cf. (2c)). Along the same lines of reasoning the equations (2) were guessed by Lee [17] for $\nu = 0$. By including the full mean curvature in (2c) we have gone beyond the leading order asymptotics to exactly reproduce the static shape of a hanging drop suspended from an orifice. As an additional benefit, the most dangerous short-wavelength instabilities of the leading order model $p = 1/h$ have been removed. In fact, the leading order model is elliptic for $\nu = 0$ [18,19] and is thus ill-posed as an initial value problem.

In [7,13] a finite difference scheme was developed capable of simulating (2) at very low viscosities. To resolve the small-scale structures we are interested in, it is crucial to use an adaptive scheme, both in time and space. The minimum thread radius and the maximum

gradient of h were taken as predictors where additional spatial resolution was necessary. Thus in a typical run the grid spacing at the position of the inviscid singularity was 6 orders of magnitude smaller than at the boundary of the computational domain. Since the equations at low viscosity are very sensitive to noise, grids with smoothly varying grid spacings had to be used, where the spacing did not change by more than 1 % from one grid point to the next. With these precautions, no numerical damping or dissipation had to be used, except for the physical viscosity ν .

Since we are interested in the limit of small viscosity, it would be tempting to put $\nu = 0$ in (2b) directly. However, we found that as soon as the motion is sufficiently nonlinear, our scheme developed instabilities on the scale of the grid, which caused the code to break down. Thus the inclusion of the full curvature term in (2c) is not enough to stabilize the numerical scheme. Similar short-wavelength instabilities have also been reported in [20] using a finite-element approach. On the other hand, exceedingly small amounts of viscosity are sufficient to stabilize the scheme, even though the viscous term is smaller than the others by several orders of magnitude throughout the domain. In the following, when speaking of a numerical solution of the inviscid equations, we will always refer to the *limit* of zero viscosity at *constant time*.

We also experimented extensively with other means of regularizing the inviscid equations, for example by using numerical viscosities as in [7]. In the upwind differencing scheme introduced in [7], the numerical viscosity is proportional to the grid spacing. The hope was to develop a scheme which automatically converges to the inviscid limit as one increases the resolution. Indeed, if the grid is coarse, a numerical viscosity was often sufficient to remove instabilities. But with improved resolution we always found the instabilities to return. Thus keeping a finite viscosity turns out to be the only reliable and at the same time the most physical way of dealing with the instabilities. These results indicate that the system (2) might be an ill-posed initial-value problem, in spite of the short-wavelength regularization introduced by (2c). If on the other hand the problem is well-posed, and the instabilities are a problem of the numerical scheme, the above limit of small viscosity will yield a solution

which coincides with the one defined by the inviscid (Lee's) equations.

It is clear that the slender-jet approximation represented by (2) *assumes* the existence of a single-valued function $h(z)$ and is thus not able to describe overturning as observed for three-dimensional axisymmetric, irrotational flow [9,10,5]. Thus there is no direct correspondence to the pinching solution found in [5]. It could be that the inviscid singularity described in this paper is a consequence of the three-dimensional equations overturning. On the other hand, as explained in the Introduction, our working assumption is that the inviscid limit of the Navier-Stokes equation is singular, in which case the limit of vanishing viscosity has no connection with solutions of the Euler equation. Thus the fact that full the potential flow equations show overturning has no obvious implications for the limit of of vanishing viscosity studied here. The resolution of these issues must clearly await full Navier-Stokes computations at small viscosity.

Figure 2 shows a simulation of (2) at a very large Reynolds number in a liquid bridge geometry with initial radius $r = 0.05$ and a small sinusoidal perturbation of wavelength $\lambda = 4\pi r_0$ superimposed on it. Owing to the Rayleigh instability, the bridge starts to pinch. Shown are three profiles close to the inviscid singularity, where the minimum radius has already decreased by a factor of 20. To the right of the minimum, an almost conical neck region is seen, on the other side a round drop has formed. Because of its small radius, the pressure in the flat region is high, pushing fluid over to the right. This causes the interface to perform a sliding motion, which lets the interface become steeper and steeper, since the drop cannot move appreciably owing to its large inertia. Note that the pressure goes to a value close to zero at the eventual place of the inviscid singularity, marked by an arrow.

Next we zoom in on the point around which h_z goes to infinity, marked by an arrow in Fig.2. To sufficiently resolve the singularity without letting viscosity become important, the Reynolds number is chosen to be $Re = 4.7 \cdot 10^9$, much larger than the Reynolds numbers treated in [13]. With such a small Reynolds number we are no longer able to resolve the huge range of length scales between the outer and the viscous scale, because L/ℓ_ν is now $2 \cdot 10^{19}$. However, the early stages of the evolution of the liquid bridge, where viscous effects

are still small can safely be resolved. In [13] it was demonstrated that the slope goes to infinity near the inviscid singularity and thus the singularity time t_c can be estimated from the blow-up of h_z . It follows from our scaling theory, to be presented in the next section, that $(h_z)_{max} \sim (t_c - t)^{-1}$. Thus t_c can be computed very accurately by plotting $((h_z)_{max})^{-1}$ versus time and fitting with a linear law. In Fig.3 we plot the maximum pressure gradient p_z , which drives the fluid motion, and the maximum velocity gradient as a function of $t_c - t$. It is seen that both p_z and v_z settle on a power law

$$(p_z)_{max} \sim (t_c - t)^{-1}, \quad (v_z)_{max} \sim (t_c - t)^{-1}. \quad (3)$$

The pressure gradient contains the highest (third) derivative in the problem. The fluctuations seen in the curve thus give an estimate of the amount of noise introduced by the regridding procedure. No noise is seen in the first velocity derivative, which clearly confirms the scaling given in (3). We thus see that the inviscid singularity is governed by power law scaling, which will be investigated in more detail in the next section. We made sure that for all of the evolution shown the viscous term remained small compared to other terms. Thus the observed scaling represents the inviscid limit of the equations we want to investigate.

We also considered a great variety of other initial perturbations, which changes the initial evolution of the bridge. In addition, we considered the bifurcation of a hanging drop in the presence of gravity as shown in Fig. 1. In all these different cases, we always found the same singularity with scaling (3) to be selected in the inviscid limit. Thus there is good evidence that the inviscid singularity to be described below is a universal feature of the equations, independent of initial conditions.

The equations (2) with $(\nu = 0)$ or systems very similar in structure have been used by a number of researchers [15,17,21–23,20,18,24] to describe pinching. However in Lee’s original paper [17] and most of the later work no attempt is made to resolve any detailed structure in the pinch region. For example, in units of the length of the computational domain, the grid spacing is $dx = 1/20$ in [17] and $1/50$ in [21]. For comparison, the minimum grid spacing used in the present paper is $dx_{min} = 10^{-10}$. In most papers [17,21,22,20] the computation

is stopped at h_{min} between 1/10 and 1/20 of the initial radius, when the position of the minimum and the drop size can be faithfully estimated. In [20], which uses a finite element code, the computations were stopped when numerical instabilities on the scale of the grid were observed. A spectral method is used in [24], but the computation was stopped at $h_{min} = 0.3$ due to numerical problems. Thus our finding of a short-wavelength instability of the inviscid equations is consistent with other numerical work, using a variety of different methods. It remains to be seen whether the inviscid versions of the Cosserat model [21] or other asymptotic models [24] are more well behaved.

III. INVISCID SIMILARITY SOLUTION

We have seen in the previous section that derivatives grow sharply near the inviscid singularity, while on the other hand the height and the velocity remains finite. This means that the similarity ansatz of [1] has to be generalized to include a “background” height and velocity profile, which is slowly varying on the scale of the singular part. At the same time, the singularity may be moving with some speed V_s , which is not necessarily the speed V with which it is convected. Thus one ends up with the similarity form

$$h(z', t') = H + t'^{\alpha} f \left(\frac{z' + V_s t'}{t'^{\beta}} \right) \quad (4)$$

$$v(z', t') = V + t'^{\alpha} g \left(\frac{z' + V_s t'}{t'^{\beta}} \right),$$

where

$$z' = z - z_c \text{ and } t' = t_c - t \quad (5)$$

measures the spatial and temporal distance from the singularity, respectively. On the spatial scale on which the inviscid singularity develops, H , V , and V_s are approximately constant. Note that (5) has self-similar form, which is superimposed on a traveling wave solution. Also, we assumed $h(z', t')$ and $v(z', t')$ to have the same scaling exponents, because this automatically balances the terms $h_z v$ and $v_z h$ in (2a).

For the ansatz (4) to be consistent, one needs $\alpha > 0$, so in the singular limit $t' \rightarrow 0$ one is left with the finite height H and velocity V . For the derivatives to blow up, $\beta > \alpha$. To see whether (4) solves the model equations (2), we balance the most singular terms in t' , deriving equations in the similarity variable

$$\eta = \frac{z' + V_s t'}{t'^{\beta}}. \quad (6)$$

One thus finds from (2a)

$$(\beta f' \eta - \alpha f) t'^{\alpha-1} = - \left[(V - V_s) f' + \frac{1}{2} H g' \right] t'^{\alpha-\beta}. \quad (7)$$

We expect the right hand side of (7) to make the dominant contribution, which will be the case if $\beta > 1$. This is because then the function f drops out of the equation, and the similarity equations only depend on the derivatives f' and g' . Thus both f and g are determined only up to constants, which is needed for consistency because our ansatz (4) has a free constant built in.

Consequently, the angular bracket must vanish, giving

$$g' = \frac{2(V_s - V)}{H} f', \quad (8)$$

which means that up to constants and a difference in amplitude $2(V_s - V)/H$ the profiles of the height and of the velocity are the same.

Turning to (2b) with $\nu = 0$, one finds to leading order

$$-(V_s - V)g't^{\alpha-\beta} = \left(\frac{f''}{f'^3}\right)' t'^{-2\alpha}. \quad (9)$$

Note that the term on the left corresponds to the highest derivatives in p_z as given by (2c). Balancing the left and the right hand side, one finds the scaling law

$$\beta = 3\alpha. \quad (10)$$

Combining (8) and (9), the similarity equation reads

$$-af' = \left(\frac{f''}{f'^3}\right)', \quad (11)$$

where $a = 2(V_s - V)^2/H$. Evidently, the constant a can be eliminated by the transformation

$$\phi(\eta) = a^{-1/3}f'(\eta). \quad (12)$$

The most general solution of the equation for ϕ ,

$$-\phi = \left(\frac{\phi'}{\phi^3}\right)', \quad (13)$$

has the form

$$\phi(\eta) = \phi_0 F[\phi_0^{3/2}(\eta - \eta_0)], \quad (14)$$

where $F(\xi)$ is a particular solution of (13).

Equation (11) can easily be solved using standard [25] tricks. In view of the freedom implied by (14), we choose $F(\xi)$ to have its maximum at $\xi = 0$, and to fall off to $1/2$ at $\xi = \pm 1/2$. Then F is given implicitly by

$$\xi = \frac{1}{8F^{3/2}}(1 + 2F)(1 - F)^{1/2}. \quad (15)$$

This function is represented in Fig. 4 as the solid line. It decays to zero like $\xi^{-2/3}$ at infinity. In view of the similarity form (4) this ensures that the leading dependence on t' drops out

far away from the singular point. This is necessary for the solution to match onto the slowly varying background field.

We note that the singularity described above is not just kinematic in nature, since a contribution from the capillary forcing enters the dominant balance in (9). In addition, the form (4) of the singularity with $V_s \neq V$ implies that it is also a traveling wave. Surprisingly, the local shape (15) of the first derivative of the local radius is identical to that of a scaling solution $h = t'G(z'/t'^{3/2})$ of the simple kinematic wave $\partial_t h + h\partial_z h = 0$ [26]. This can be checked directly from the similarity equation for $G(\xi)$. At present we do not know if this is a coincidence or is the result of a deeper analogy.

To test the prediction of the theory, we took the same simulation as in Fig. 3 at a time where the slope was $h_z = 10^4$. We included the profile of h_z in Fig. 4, shifting the maximum to the origin and normalizing its width. It is evident that our analytical theory is fully confirmed by the comparison. The free constants ϕ_0, η_0 in (14) and the parameter a in (11) are not determined by the similarity theory. Indeed, we confirmed that they depend on initial conditions and therefore cannot come out of a local theory.

Our next concern is to find the scaling exponents α and β , which are not determined from dimensional reasoning as in [1], but which are constraint by the scaling relation (10). In addition, (11) does not depend on the values of the exponents, so α cannot be selected by properties of the similarity equation, as was the case in [27]. To investigate this problem, we must look at next to leading order terms such as the ones contained in Eq. (7). Correspondingly, there are sub-leading terms in h and v , which have the form

$$h(z', t') = H + t'^\alpha f\left(\frac{z' + V_s t'}{t'^\beta}\right) + t'^{2\alpha} f_1\left(\frac{z' + V_s t'}{t'^\beta}\right) + \dots, \quad (16)$$

and correspondingly for $v(z', t')$. Then (2a) becomes to next to leading order:

$$[3\alpha f' \eta - \alpha f] t'^{\alpha-1} = \left[-g f' - \frac{1}{2} f g' + (V_s - V) f'_1 - \frac{H}{2} g'_1\right] t'^{-\alpha}. \quad (17)$$

Since the terms must balance, we get

$$\alpha = \frac{1}{2}, \quad \beta = \frac{3}{2}, \quad (18)$$

which are the desired exponents. Note that this conforms with the scaling of both the pressure and the velocity gradient from (3), since

$$p_z \approx t'^{-2\alpha} \left(\frac{f''}{f'^3} \right)' \quad \text{and} \quad v_z \approx t'^{\alpha-\beta} g'. \quad (19)$$

Thus both the value of the exponents and the shape of the profiles is in excellent agreement with theory.

IV. DISCUSSION

In [13] we have studied the steepening of the height profile for small but finite viscosities. The slopes saturate at a large value, the maximum slope roughly following a scaling law $(h_z)_{max} \sim Re^{1.25}$. As long as the viscous term is much smaller than the pressure gradient, one can use the inviscid similarity solution. The naive expectation is that the slope saturates as soon as the viscous term is of the same order as the pressure gradient. Using (4) and (18), the temporal scaling of the pressure gradient is $p_z \sim t'^{-1}$ and that of the viscous term $Re^{-1}(v_z h)_z/h^2 \sim Re^{-1}t'^{-5/2}$, where $Re^{-1} = \nu/(UL)$ is constant. Equating the two we find $(h_z)_{max} \sim Re^{2/3}$, which is far too small an exponent. A possible explanation is that the Reynolds numbers for which the exponent 1.25 was found are still too small. But more likely there is an intricate interplay between the inviscid singularity and viscosity, leading to a more complicated intermediate scaling range. Indeed, for the Reynolds numbers considered, the slope continues to grow far beyond the time where the pressure gradient first balances the viscous term at a point. It thus remains a challenge to find the mechanism which makes the slope saturate.

The pinching of vortex sheets and jets within the framework of inviscid hydrodynamics has recently been the object of much scrutiny [28–30]. The motion is either driven by surface tension, or comes from the flow field generated by the regions of high vorticity. Short wavelength instabilities arise just as in our problem, which are usually removed by filtering out high-wavenumber components of the Fourier spectrum [31]. It would be interesting to

see whether this is equivalent to adding a small amount of viscosity, which is the physical regularization used in the present paper. It is not clear that Krasny filtering actually selects the physical solution. So far, analytical solutions have not been found for the singular motion of vortex sheets or lines. It remains to be seen whether the singularity structure found in the present problem carries over.

We have seen that the slender-jet model (2) in the limit of small viscosity is characterized by more than just the scale of the minimum radius. Instead, a shock-type singularity develops whose width represents another, much smaller scale. The crucial question is of course whether a similar mechanism is at work in the small-viscosity limit of the Navier-Stokes equation, which could make this limit singular. It is unlikely that the three-dimensional equation has precisely the same spatial singularity structure than the one found in the model equations, which constrain axial velocity gradients to a far greater extent. Instead it is probable that high-pressure fluid in the neck is injected into the drop, a situation which is only poorly captured by the slice average of the model. The Navier-Stokes equation might thus form a very thin boundary layer around the jet, in which viscosity remains important even for arbitrarily small ν . This is a possible scenario which would invalidate the purely inviscid calculation of [5], at least from a physical point of view.

Even for the model equations, many unanswered questions remain. It is fascinating that even a simple one-dimensional model is capable of such complexity, the key to its understanding lying in the analysis of the singularities.

ACKNOWLEDGMENTS

I have benefited greatly from discussions with Michael Brenner. This work is partially supported by the Deutsche Forschungsgemeinschaft through Sonderforschungsbereich 237.

REFERENCES

- [1] J. Eggers, “Universal Pinching of 3D Axisymmetric Free-Surface Flow,” *Phys. Rev. Lett.* **71**, 3458 (1993).
- [2] X. D. Shi, M. P. Brenner, and S. R. Nagel, “A Cascade Structure in a Drop Falling from a Faucet,” *Science* **265**, 157, (1994)
- [3] T. A. Kowalewski, “On the separation of droplets from a liquid jet”, *Fluid Dyn. Res.* **17**, 121 (1996).
- [4] J. Eggers, “Nonlinear dynamics and breakup of free-surface flows”, *Rev. Mod. Phys.* **69**, 865 (1997).
- [5] R. F. Day, E. J. Hinch, and J. R. Lister, “Self-similar Capillary Pinchoff of an Inviscid Fluid”, *Phys. Rev. Lett.* **80**, 704 (1998).
- [6] D. H. Peregrine, G. Shoker, and A. Symon, “The bifurcation of liquid bridges,” *J. Fluid Mech.* **212**, 25 (1990).
- [7] J. Eggers and T. F. Dupont, “Drop Formation in a One-Dimensional Approximation of the Navier-Stokes Equation,” *J. Fluid Mech.* **262**, 205 (1994).
- [8] R. Grauer, C. Marliani, and K. Germaschewski, “Adaptive mesh refinement for singular solutions of the incompressible Euler equations”, *Phys. Rev. Lett.* **80**, 4177 (1998).
- [9] N.N. Mansour and T. S. Lundgren, “Satellite formation in capillary jet breakup”, *Phys. Fluids* **2**, 114, (1990).
- [10] R. M. S. M. Schulkes, “The evolution and bifurcation of a pendant drop”, *J. Fluid Mech.* **278**, 83, (1994).
- [11] Y.-J. Chen and P. H. Steen, “Dynamics of inviscid capillary breakup: collapse and pinch-off of a film bridge”, *J. Fluid Mech.* **341**, 245 (1997).

- [12] N. Ashgriz and F. Mashayek, “Temporal analysis of capillary jet breakup”, *J. Fluid Mech.* **291**, 163, (1995).
- [13] M. P. Brenner et al., “Breakdown of scaling in droplet fission at high Reynolds numbers”, *Phys. Fluids* **9**, 1573 (1997).
- [14] J. B. Keller and M. J. Miksis, “Surface Tension Driven Flows,” *SIAM J. Appl. Math.* **43**, 268 (1983).
- [15] L. Ting and J. B. Keller, “Slender jets and thin sheets with surface tension”, *SIAM J. Appl. Math.* **50**, 1533, (1990).
- [16] S. E. Bechtel, M. G. Forest, and K. J. Lin, “Closure to all orders in 1-D models for slender viscoelastic free jets: An integrated theory for axisymmetric, torsionless flows,” *SAACM* **2**, 59 (1992).
- [17] H. C. Lee, “Drop formation in a liquid jet”, *IBM J. Res. Develop.* **18**, 364 (1974).
- [18] D. T. Papageorgiou, “Analytical description of the breakup of liquid jets”, *J. Fluid Mech.* **301**, 109 (1995).
- [19] M. A. Fontelos and J. J. L. Velázquez, “On the breakup of thin fluid tubes”, submitted.
- [20] R. M. S. M. Schulkes, “Nonlinear dynamics of liquid columns: A comparative study”, *Phys. Fluids. A* **5**, 2121 (1993).
- [21] J. Meseguer, “The breaking of axisymmetric slender liquid bridges”, *J. Fluid Mech.* **130**, 123, (1983).
- [22] J. Meseguer and A. Sanz, “Numerical and experimental study of the dynamics of axisymmetric slender liquid bridges”, *J. Fluid Mech.* **153**, 83, (1985).
- [23] R. M. S. M. Schulkes, “Dynamics of liquid jets revisited”, *J. Fluid Mech.* **250**, 635 (1992).

- [24] D. T. Papageorgiou and O. Orellana, “Study of cylindrical jet breakup using one-dimensional approximations of the Euler equation”, preprint.
- [25] C. M. Bender and S. A. Orszag, *Advanced mathematical methods for scientists and engineers*, (Mc Graw-Hill, N. Y., 1978).
- [26] I am grateful to an anonymous referee for this remark.
- [27] Ch. Uhlig and J. Eggers, “Singularities in cascade models of the Euler equation”, *Z. Phys. B* **103**, 69 (1997).
- [28] R. E. Caflisch, X. Li, and M. J. Shelley, “The collapse of an axi-symmetric, swirling vortex sheet”, *Nonlinearity* **6**, 843 (1993).
- [29] M. C. Pugh and M. J. Shelley, “Singularity Formation in Models of Thin Jets with Surface Tension”, *Comm. Pure Appl. Math.* **51**, 733 (1998).
- [30] J. Lowengrub and L. Truskinovski “Quasi-incompressible Cahn-Hilliard Fluids and Topological Transitions”, *Proc. Roy. Soc. London*, submitted
- [31] R. Krasny, “A study of singularity formation in a vortex sheet by the point-vertex approximation”, *J. Fluid Mech.* **167**, 65 (1986).

FIGURES

FIG. 1. A drop of water falling from a faucet 0.51cm in diameter. The lines represent a computation using one-dimensional model equations. This figure is taken from [7].

FIG. 2. A closeup view of simultaneous radius, velocity, and pressure profiles close to the inviscid singularity. The Reynolds number is $Re = 5 \cdot 10^9$, and the time between successive profiles is $5 \cdot 10^{-5}$. The arrow marks the asymptotic location of the shock.

FIG. 3. The maximum of the gradient of the pressure and of the velocity as function of the time distance from the inviscid singularity. The Reynolds number is $4.7 \cdot 10^9$. Both curves asymptote to a slope very close to -1 .

FIG. 4. The normalized similarity function $F(\xi)$, cf. (12), (14).

Figure 1

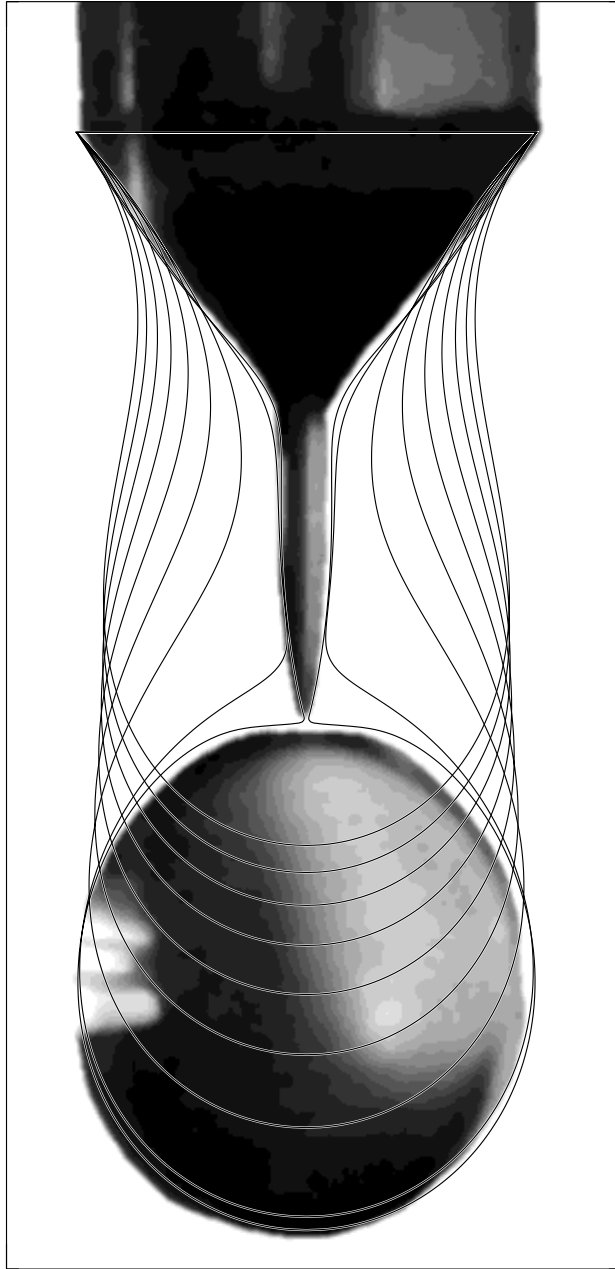


Figure 2

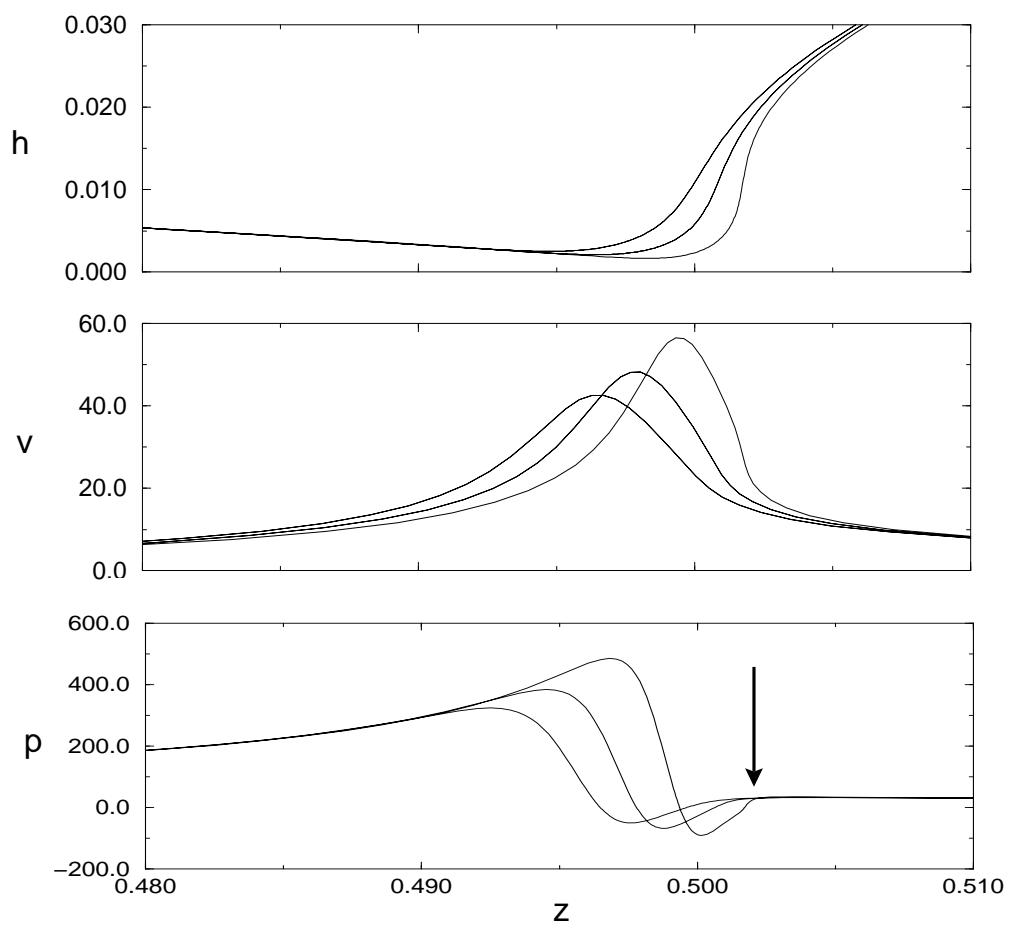


Figure 3

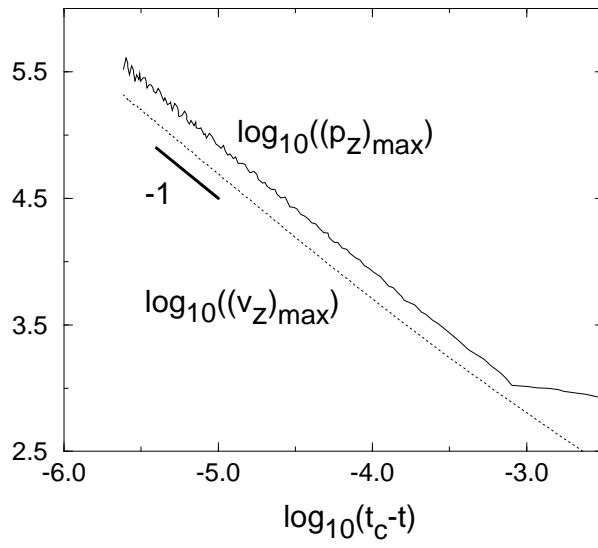


Figure 4

